Journal of Cleaner Production 392 (2023) 136256

Contents lists available at ScienceDirect

Journal of Cleaner Production

journal homepage: www.elsevier.com/locate/jclepro

Considerable role of urban functional form in low-carbon city development

Ting Lan [a], Guofan Shao [b], Zhibang Xu [a], Lina Tang [a,*], Hesong Dong [a,c]

[a] Key Laboratory of Urban Environment and Health, Institute of Urban Environment, Chinese Academy of Sciences, Xiamen, 361021, China
[b] Department of Forestry and Natural Resources, Purdue University, West Lafayette, IN 47907, USA
[c] University of Chinese Academy of Sciences, Beijing 100049, China

ARTICLE INFO

Handling Editor: Lei Shi

Keywords:
CO_2 emissions
Urban functional form
China
Low-carbon cities
Urban compactness

ABSTRACT

Urban form, especially urban functional form, is an important consideration for urban planning, construction, and management. Recent progress in characterizing urban functional form makes it possible to quantify the relationship between urban functional form and urban carbon emissions. We used urban functional form data from 178 cities of China to study the relationship between urban CO_2 emissions and five categories of urban form: compactness, extension, fragmentation, irregularity, and concentration. The results show that all five categories significantly affect the total CO_2 emissions (TCE), and four categories (excluding fragmentation) significantly affect per-capita CO_2 emissions (PCE). Compactness produces a significant negative effect on both TCE and PCE: for every 1% increase in the functional compactness index (FCI), TCE and PCE decrease by 0.79% and 0.34%, respectively. Carbon-emission-reduction policies should be combined with the topographical environment, spatial structure, and industrial structure of cities. FCI reduces carbon emissions most effectively in plain and single-center cities. The planning and control of forms are more important in hilly and mountainous cities, multi-center cities, and highly industrial cities. This study concludes that the adjustment of urban functional form has important theoretical and practical significance for low-carbon city development.

1. Introduction

Climate change caused by global warming poses tremendous challenges to the sustainable development of human society. It triggers numerous environmental issues such as urban heat islands, rising sea levels, frequent extreme weather events, plant and animal reduction, etc. (Clark et al., 2016; Smith et al., 2015; Tollefson, 2021). The cumulation of carbon dioxide (CO_2) emissions is the primary culprit for global warming (Hansen and Lebedeff, 1987). Cities, as the fastest growing human habitats on Earth, contribute over 70% of global CO_2 emissions (GEA, 2012; IEA, 2012; Kennedy et al., 2014; Wang et al., 2019a). Reducing CO_2 emissions, especially in cities, is essential for the sustainable development of cities and of human society (Khanna et al., 2014; Rosenzweig et al., 2010; Zhang et al., 2014).

Widely known methods to reduce carbon emissions include adjusting energy structure, developing non-fossil energy, inventing negative-emission technology, setting up low-carbon pilot cities, and establishing green markets (Liu et al., 2021b). It is noteworthy that the relationship between urban form and CO_2 emissions has received increasing attention (Cai et al., 2021; Fang et al., 2015; Li et al., 2022; Wang et al., 2019a).

A growing number of studies show that urban form strongly affects the level of CO_2 emissions (Liu et al., 2014, 2020; Makido et al., 2012; Zuo et al., 2022). For example, Wang et al. (2017) analyzed how socioeconomic factors, urban form, and transportation networks affect CO_2 emissions in China's megacities and reported that fragmentation and irregularity of urban form increase CO_2 emissions. Ou et al. (2013) examined the relationship between carbon emissions and urban form from 1990 to 2010 by taking the four fastest-growing Chinese cities (Beijing, Shanghai, Tianjin, and Guangzhou) as examples and found that the increase of urban area increases CO_2 emissions, as does land fragmentation and irregularity. Fang et al. (2015) studied the relationship between urban form and CO_2 emissions of 30 provincial capital cities in China and drew similar conclusions. Bereitschaft and Debbage (2013) reported that, when population, land area, and climate were controlled, greater urban sprawl in U.S. metropolitan areas was associated with greater air pollution and CO_2 emissions. In a study of European cities, researchers found that high urban patch fragmentation and dense urban patches correlated with low greenhouse gas emissions (Baur et al., 2015). Cirilli and Veneri (2013) explored the relationship between the

* Corresponding author. Institute of Urban Environment, Chinese Academy of Sciences, 1799 Jimei Road, Xiamen 361021, China.
E-mail addresses: tlan@iue.ac.cn (T. Lan), shao@purdue.edu (G. Shao), zbxu@iue.ac.cn (Z. Xu), lntang@iue.ac.cn (L. Tang), hsdong@iue.ac.cn (H. Dong).

https://doi.org/10.1016/j.jclepro.2023.136256
Received 8 November 2022; Received in revised form 2 January 2023; Accepted 29 January 2023
Available online 31 January 2023
0959-6526/

spatial structure of 111 urban areas in Italy and the CO_2 emissions generated by commuting and found that the smaller, more compact cities with fewer urban centers produced less CO_2 emissions per resident from commuting. Wang et al. (2018a) studied how urban form affects CO_2 emission in the Pearl River Delta, China, and found that urban compactness significantly reduces CO_2 emission efficiency and that compact urban form can effectively improve CO_2 emission efficiency. However, opposing views argue that urban form plays only a small role in reducing CO_2 emissions (Gaigne et al., 2010).

As mentioned above, researchers have investigated the relationship between urban form and CO_2 emissions in different countries and regions, and the most common metrics of urban form are size, expansion, complexity, irregularity, and urban compactness (Guo et al., 2022; Shi et al., 2020; Wang et al., 2018a). In previous studies, the term "urban form" mainly refers to the urban physical form, i.e., the physical characteristics of the built-up areas, including the shape, size, expansion, and configuration of urban areas (Thinh et al., 2002; Williams, 2014). However, given that cities are giant, complex systems, urban functional form is also an important aspect of urban form (Thinh et al., 2002) and may also play a key role in achieving low-carbon cities (Cao et al., 2022; Wang et al., 2018b). Urban functional form is the functional characteristics that make up the configuration of urban areas and consists of the interaction between the internal order of the city and the external environment (Lan et al., 2021). The difficulty of acquiring data on urban functional attributes over a large scale has led to a lack of research on the relationship between the urban functional form and CO_2 emissions. Therefore, based on existing research, we explore herein the relationship between urban and CO_2 emissions in multiple categories by considering urban functional form as an important indicator of urban compactness. The scientific questions addressed herein are (i) how do different categories of urban form, especially urban functional form, relate to CO_2 emissions? (ii) Which category of urban form is more conducive to reducing carbon emissions? (iii) How strongly does urban form contribute to low-carbon cities?

2. Study area

China is a vast country with diverse and complex urban types (Jiao et al., 2020), forming a rich environment in which to explore the relationship between urban form and CO_2 emissions in multiple categories (Liu et al., 2021b; Yao et al., 2021). This work considers 178 case cities (Fig. 1) that all have a certain urban scale and an urban permanent resident population of over 400 000, where the population data were

Fig. 1. Location of sample cities.

obtained from the *China Construction Statistical Yearbook*. The case cities are of different sizes: five megacities (urban permanent resident population >10 million), nine extra-large cities (urban permanent resident population of 5–10 million), 78 large cities (urban permanent resident population of 1–5 million), 60 medium cities (urban permanent resident population between 0.5 and 1.0 million), and 26 small cities (urban permanent resident population less than 0.5 million). Additionally, the case cities have different administrative levels: four municipalities are directly controlled by the central government, five cities are specifically designated in the state plan, 26 cities are provincial capitals, and 143 cities are prefecture-level cities. In terms of population, the national urban population is 409 757 200, and the total urban permanent resident population of the 178 case cities is 297 576 700, which is 73% of the national urban population. Thus, the results of this study are representative of the relationship between urban form and carbon emissions in these 178 cities.

3. Materials and methods

3.1. CO_2 emission data

There are two broad approaches to estimating CO_2 emissions, the first method is based on the inventory factor proposed by the Intergovernmental Panel on Climate Change (Fang et al., 2015), but this method only provides CO_2 emission data on the administrative scale as opposed to a finer spatial scale. The second method is to invert CO_2 emissions by combining nighttime-light remote-sensing data (Liu et al., 2018). The CO_2 emissions data used herein comes from the Open-Data Inventory for Anthropogenic CO_2 (ODIAC), which provides high-spatial resolution (1 km × 1 km) gridded global data on CO_2 emissions from fossil fuel combustion (Oda and Maksyutov, 2011). ODIAC data are calculated by combining multi-source nighttime lighting data with the global point source carbon emissions database and ship and aircraft tracks. It has been widely used in many studies, such as for estimating urban emissions and monitoring system-design experiments (Oda et al., 2018; Shi et al., 2020). Studies have shown that these data accurately allocate CO_2 emissions on global, regional, national, and city scales. ODIAC has several versions, and we use herein the sum of the 12 months in 2019 of carbon emissions data as the annual total CO_2 emissions (TCE) for 2019, which is provided by the ODIAC 2020 data product. The TCE for each city is obtained from the sum of CO_2 emissions within the urban area in this paper.

The intensity of CO_2 emissions is usually expressed in three ways: per capita CO_2 emissions (PCE), per unit area CO_2 emissions, and per GDP CO_2 emissions (Sha et al., 2020). The PCE is obtained by dividing the total urban CO_2 emissions by the total population within the urban area, which minimizes any bias due to urban size. We use the PCE herein to express the intensity of urban CO_2 emissions in this work and calculate it as follows:

$$\mathrm{PCE} = \mathrm{TCO_2}/P, \tag{1}$$

where TCO_2 is the total CO_2 emissions within the urban area, and P is the total resident population in the urban area.

3.2. Urban area and urban functional zone

The urban extent (UE) from the global hierarchical urban boundaries produced by Xu et al. (2021) is used to quantitatively assess the characteristics of urban form. The UE contains some open spaces and water, and since these areas contain few points of interest (POI), it is difficult to determine the functional attributes of these areas. Therefore, we combined the POI to adjust the scope of UE and obtain the final research boundaries. The specific methods are detailed in previous work (Lan et al., 2021).

Urban functional form, expressed in terms of urban functional compactness index (FCI), serves as an important indicator of compactness. FCI takes street blocks as the basic analysis unit and mainly considers the functional zoning and the intensity of human activity to assess the rationality of the functional layout of cities. The data used to calculate the urban FCI include three items: (1) POI, which were obtained from A map (a Chinese internet map company: https://www.amap.com/) in 2019; (2) road networks obtained from Openstreet map (a free, open source, editable mapping service: https://www.openstreetmap.org/) in 2019; and (3) nighttime-lights data. The Earth Observation Group produced a V.2 annual time series of global VIIRS nighttime lights (Annual VNL V2) based on monthly averages acquired with filtering to remove extraneous features such as biomass burning, aurora, and background noise (Elvidge et al., 2021). This work uses the 2019 nighttime lights. Details regarding the data are available in previous publications (Lan et al., 2021; Sun et al., 2019).

3.3. Urban form metrics

Urban form is the spatial configuration of fixed elements in an urban area (Anderson et al., 1996) and is portrayed via multiple categories (Liu et al., 2021a), such as urban extension, irregularity, fragmentation, and compactness. The latter includes two basic aspects: physical compactness and functional compactness (Thinh et al., 2002). Urban physical compactness of urban space generally refers to the concentration or compactness of urban physical forms such as urban areas, the impervious surface of cities, or the strong correlation between parcels. Urban functional compactness refers to the effective mixing of the various functional zones in a city so as to maximize the functional benefits of a given plot.

Following previous studies (Makido et al., 2012; Shi et al., 2020; Wang et al., 2018a), we selected eight indicators to portray urban form in five categories: compactness (physical compactness and functional compactness), extension, fragmentation, irregularity, and concentration. Two indicators are chosen to represent the compactness of cities: The first is the physical compactness index (CI), which is based on the formula of gravity (Thinh et al., 2002), and the second is the FCI, which is further developed starting from the CI (Lan et al., 2021). The larger the FCI and CI, the more compact the city. Urban expansion, fragmentation, irregularity, and concentration are represented by various landscape metrics (Jia et al., 2019). Urban expansion is characterized by total area (TA), where greater TA corresponds to greater urban expansion. Urban fragmentation is expressed by the largest patch index (LPI), which correlates negatively with urban fragmentation. Urban irregularity is characterized by the landscape shape index (LSI) and the mean perimeter-area ratio (PARA_MN); the larger the LSI and PARA_MN, the more complex the city. The patch cohesion index (COHESION) and effective mesh size (MESH) represent the concentration of patches; the larger the COHESION and MESH, the more concentrated the urban patches. Table 1 gives the definitions and formulas for the urban form metrics.

3.4. Regression model

The ordinary least squares (OLS) regression model is one of the most used regression models. It assumes that the regression parameters are consistent across regions and does not consider spatial nonstationarity due to changes in the relationship between variables or changes in structure caused by changes in geographic location. In 1996, Fotheringham proposed the geographically weighted regression (GWR) model, which considers the information of geographic location based on the linear regression model and estimates local regression parameters by using the weighted least squares method. The formula for GWR is

$$y_i = \beta_0(u_i, v_i) + \sum_{j=1}^{k} \beta_k(u_i, v_i) x_{ik} + \varepsilon_i, \tag{2}$$

where y_i is the total CO_2 emissions of city i, $\beta_0(u_i, v_i)$ is an intercept term, $\beta_k(u_i, v_i)$ is the regression coefficient of the independent variable k in city i, (u_i, v_i) is the longitude and latitude coordinates of city i, x_{ik} is the value of the independent variable k for city i, and ε_i is the residual of city i. The golden_search method is used to calculate the neighborhood, the continuous Gaussian kernel function is used to calculate the spatial weight coefficients, and the bisquare is used for the local weighting scheme.

Table 1
Description of urban form indicators used in the study.

Category	Indicator	Equation	Description
Compactness	Functional compactness Index (FCI)	$F_{RX} = \frac{1}{MN}\sum_{i\in\varphi_i}\sum_{j\in\varphi_j}\frac{1}{c}\frac{R_i X_j}{d^2(i,j)}$ $\mathrm{FCI} = \sum F_{RX}$ ($X =$ 2,3,4,5)	F_{RX} = spatial gravitation between the intensity of human activity of the residential zone and that of another zone; φ_i = set of point i, φ_j = set of point j; R_i = intensity of human activity of point i in the residential zone; X_j = intensity of human activity of point j in class X; d = Euclidean distance between point i and point j; M = total number of points in the residential zone; N = total number of points in any of the other four classes; $c = 100$ (nW cm^{-2} sr^{-1})^2 m^{-2}.
	Physical compact Index (CI)	$CI = \frac{\sum \frac{1}{c}\frac{Z_i Z_j}{d^2(i,j)}}{N(N-1)/2}$	Z_i, Z_j = urban areas in cells i and j ($i \neq j$); $d\,(i, j)$ = Euclidean distance (m) between cells i and j; $c = 100$ (m^2); N = total number of cells.
Extension	Total areas (TA)	$TA = \sum_{j=1}^{n} a_{ij}(1/10000)$	a_{ij} = area (m^2) of patch ij.
Fragmentation	The largest patch index (LPI)	$\mathrm{LPI} = \frac{\mathrm{Max}(a_j)}{N} \times 100$	a_j = area (m^2) of urban patch j in terms of number of cells; N = total number of patches.
Irregularity	Landscape shape index (LSI)	$\mathrm{LSI} = \frac{0.25\sum_{k=1}^{m} e_{ik}^{*}}{\sqrt{TA}}$	e_{ik}^{*} = total length (m) of edge in landscape between class i and k; TA = total landscape areas (m^2).
	Mean perimeter-areas ratio (PARA_MN)	$\mathrm{PARA\_MN} = \frac{\sum_{i=1}^{m}\sum_{j=1}^{n}\frac{p_{ij}}{a_{ij}}}{N}$	p_{ij} = perimeter (m) of patch ij; a_{ij} = area (m^2) of patch ij; N = total number of patches.
Concentration	Patch cohesion index (COHESION)	$\mathrm{COHSION} = 100\left[1 - \frac{\sum_{i=1}^{m}\sum_{j=1}^{n} p_{ij}^{*}}{\sum_{i=1}^{m}\sum_{j=1}^{n} p_{ij}^{*}\sqrt{a_{ij}^{*}}}\right] * \left[1 - \frac{1}{\sqrt{Z}}\right]^{-1}$	p_{ij}^{*} = perimeter of patch ij in terms of number of cells; a_{ij}^{*} = area of patch ij in terms of number of cells; Z = total number of cells in the landscape.
	Effective mesh size (MESH)	$\mathrm{MESH} = \frac{\sum_{j=1}^{n} a_{ij}^{2}}{TA}\left(\frac{1}{10000}\right)$	TA = total landscape areas (m^2); a_{ij} = area (m^2) of patch ij.

The determination of bandwidth is important in the GWR model because it determines how many observations are included near each city in the matrix. In this work, the optimal bandwidth is determined by the corrected Akaike information criterion (AICc) (Wang et al., 2019b).

4. Results

4.1. Spatial heterogeneity of urban form in Chinese cities

The eight urban form indicators were divided into five categories based on the nature breaks (Jenks) method.

Spatial characteristics of urban compactness. For cities in different economic zones, significant differences appear in the FCI, with the general rule for FCI being that it is higher in the north and lower in the south. Significant differences also appear between northeastern and eastern cities, western cities, and central cities. The FCIs of northeastern cities are significantly greater than those of the other three economic zones, and the FCIs of eastern, western, and central cities are similar to each other [Figs. 2(a) and 3(a)]. Of the four economic regions, the FCIs of cities in the northeast are the highest, with an average of 43.14, followed by the northern cities, with an average of 22.91, then by the central cities, with an average of 13.98, and finally by the eastern cities, with an average of 11.19. The CIs of cities follow the general rule of being higher in the north and lower in the south, and higher in the west and lower in the east. The CIs of eastern cities differ significantly from those of the other three major economic zones. The CIs of eastern cities are smaller, and the CIs of western cities, central cities, and northeastern cities are all similar to each other [Figs. 2(b) and 3(b)].

Spatial characteristics of urban extension. The cities with greater urban expansion are mainly provincial capitals and are concentrated in the eastern region. The TA of these cities is spatially distributed as follows: eastern (average TA is 22 774.40) > western (10 740.31) > central (8491.06) > northeastern (7324.10). The TA of eastern cities is significantly greater than that of the cities in the other three economic regions, and the TA of western, central, and northeastern cities are all similar to each other (Figs. 2(c) and 3(c)).

Spatial characteristics of urban fragmentation. The LPIs of eastern cities average 69.03 and are significantly smaller than those of the cities in the remaining three economic regions, which average 82.89, 82.45, and 81.82 for the central, northeastern, and western cities, respectively.

Spatial characteristics of urban irregularity. The LSIs of eastern cities average 7.89 and are more dispersed and different significantly from the LSIs cities in the other three economic regions, which average 4.22, 4.54, and 5.13 for the northeastern, central, and western cities, respectively [cf. Figs. 2(e) and 3(e)]. In addition, PARA_MN for eastern cities significantly exceeds that for western cities. Ranking the regions in terms of mean PARA_MN gives northeast (800.54) > eastern (798.17) > central (766.03) > western (634.02) [Figs. 2(f) and 3(f)].

Spatial characteristics of urban concentration. The range of COHESION is small, and the difference between cities in four regions is not significant [Figs. 2(g) and 3(g)]. The MESH of eastern cities and some provincial capitals is larger, but no significant difference exists between cities in the four regions [Figs. 2(h) and 3(h)].

4.2. Spatial heterogeneity of CO_2 emissions in Chinese cities

The TCE in Chinese cities is generally higher in the east and lower in

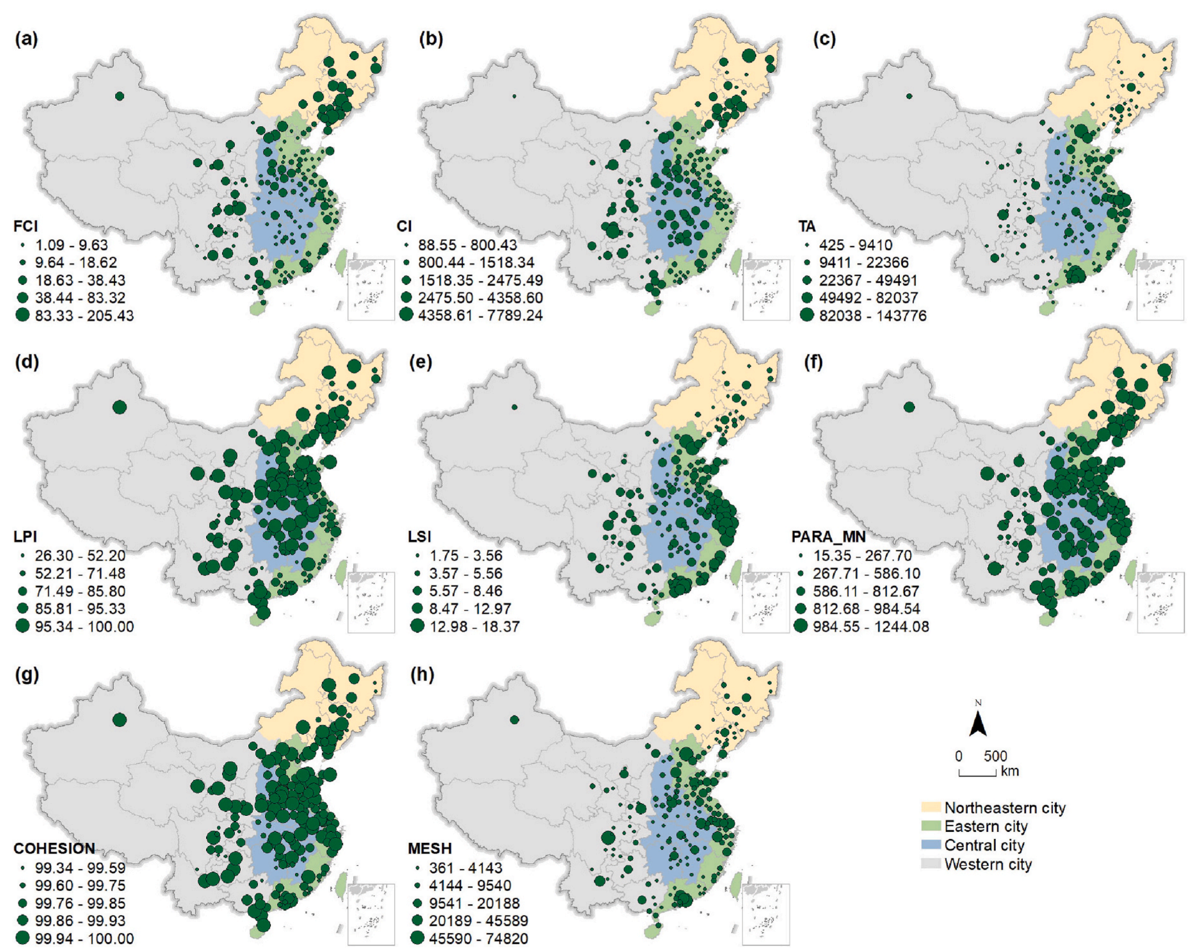

Fig. 2. Spatial distribution of the eight form indicators of the study.

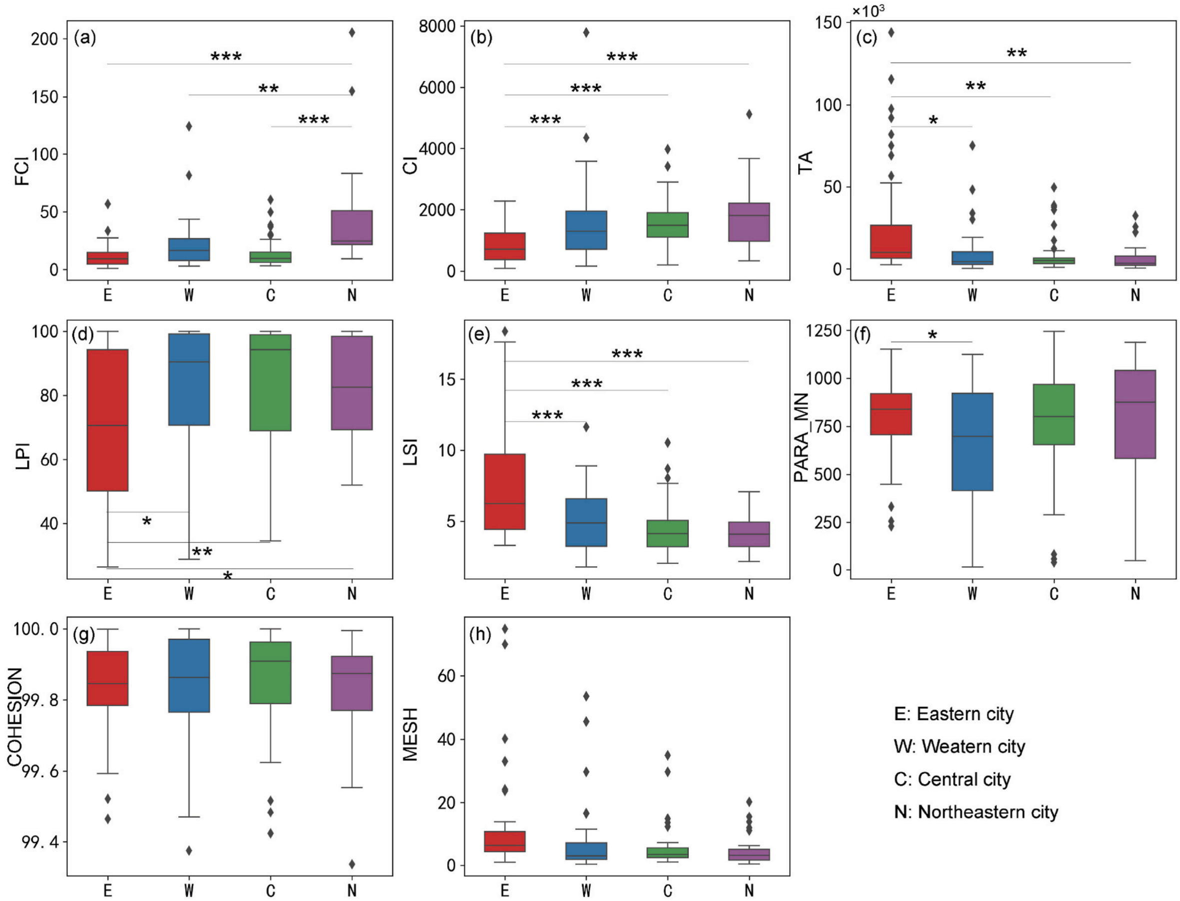

Fig. 3. Boxplots of the eight form indicators for the different economic zones. Note: *, **, and *** indicate that the results are significant at the 0.05, 0.01, and 0.001 levels, respectively.

the west, and the cities with larger TCE are mainly concentrated in the Beijing-Tianjin-Hebei urban agglomeration, the Yangtze River Delta urban agglomeration, and the Pearl River Delta urban agglomeration. Eastern cities have the largest TCE, followed by central cities, western cities, and then northeastern cities. Furthermore, cities in the eastern region have significantly greater TCE than cities in the other three economic regions [Fig. 4(a)]. The PCE is generally higher in the north and lower in the south, with more CO_2 emissions per capita in the northern cities, where coal is the main energy source, and less in the south. At the same time, larger cities have higher CO_2 emissions per capita, and the eastern cities have higher CO_2 emissions per capita than the cities in the other three economic regions. However, no significant difference appears in CO_2 emissions per capita between the four economic regions [Fig. 4(b)].

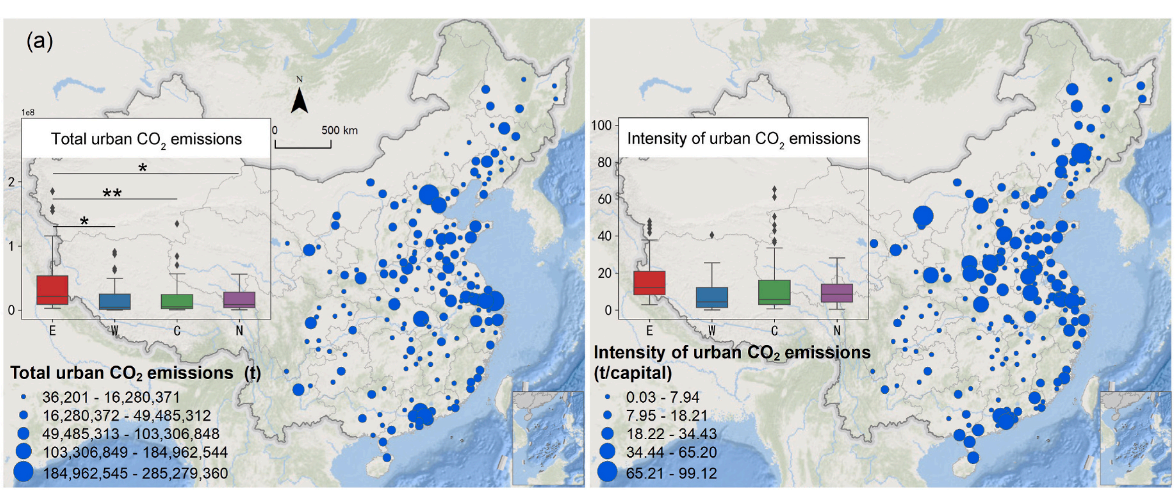

Fig. 4. Spatial characteristics of total urban CO_2 emissions and intensity of urban CO_2 emissions. Note: * (**) indicates that the results are significant at the 0.05 (0.01) level.

4.3. Relationship between urban form and CO_2 emissions on national level

First, all variables were transformed by the natural logarithm. Next, taking TCE and PCE as dependent variables and eight form indicators as independent variables, we explore the relationship between urban form and CO_2 emissions at the national level. For the relationship between TCE and urban form, all form indicators passed the significance test, but different urban form indicators produced different effects on TCE (Fig. 5). The CI accounts for 53.94% of TCE, which is greater than that of FCI, and both compactness indicators correlate negatively with TCE. For every 1% increase in CI, TCE decreases by 1.36%, and for every 1% increase in FCI, TCE decreases by 0.79% [Fig. 5(a) and (b)]. Of all form categories, the category "urban extension" explains the most of TCE, with $R^2 = 0.64$, and exhibits a strong positive correlation with TCE. For every 1% increase in TA, TCE increases by 1.17% [Fig. 5(c)]. The LPI significantly reduces TCE, implying that greater fragmentation produces more CO_2 emissions. However, the degree of fitting is relatively low, with $R^2 = 0.06$ [Fig. 5(d)]. Both indicators of urban irregularity, the LSI and PARA_MN, significantly increase TCE, implying that more complex urban forms increase TCE. However, for PARA_MN, $R^2 < 0.06$ [Fig. 5(e) and (f)]. The two indicators of urban concentration, COHESION and MESH, both exhibit a significant positive correlation with TCE; that is, an increase in urban concentration increases TCE. The range of COHESION is particularly concentrated so that the slope of ln (COHESION) and ln (TCE) reaches 257.36, but with $R^2 = 0.05$. The explanatory power of MESH for TCE, with $R^2 = 59\%$, is second only to that of TA [Fig. 5(g) and (h)].

The indicators PARA_MN and COHESION provide poor fits to the TCE and so are removed. To analyze the relationship between PCE and urban form, this leaves six indicators in five categories as independent variables and PCE as the dependent variable. Compared with TCE, the fitting quality and degree of influence of the six form indicators are reduced for PCE, and only five form indicators pass the significance test. Of these five, both indicators of compactness have a significant negative correlation with PCE, and the CI fits better and has a greater impact on PCE: each 1% increase in the CI reduces PCE by 0.51%, and each 1% increase in the FCI reduces PCE by 0.34%. Urban expansion, irregularity, and concentration positively affect PCE, with TA, an indicator of urban expansion, and MESH, an indicator of urban concentration, best explaining PCE, at 21% and 23%, respectively. Each 1% increase in TA and MESH increases PCE by about 0.50% and 0.60%, respectively. The LPI indicator, which reflects urban fragmentation, does not pass the significance test and so does not affect PCE (Fig. 6).

4.4. Relationship between urban form and CO_2 emissions on local level

The GWR model considers the spatial nonstationarity caused by changes in geographical location, assigns weights to each sample, and attributes a corresponding regression equation to each sample city. Therefore, this study uses the GWR model to analyze the relationship between urban form and TCE and PCE on the local level. After excluding

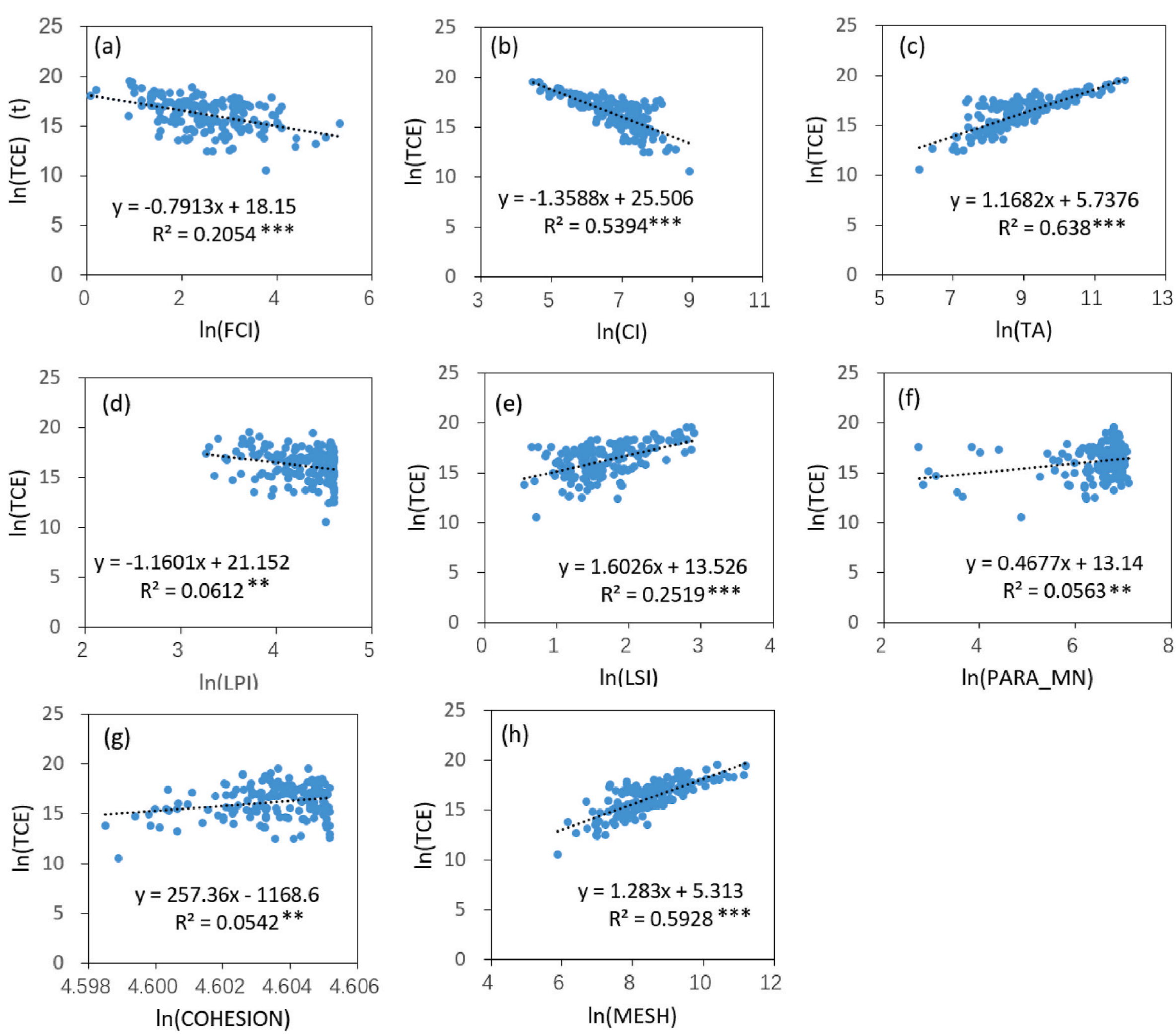

Fig. 5. Relationship between urban form indicators and TCE. Note: ** (***) indicates that the results are significant at the 0.01 (0.001) level.

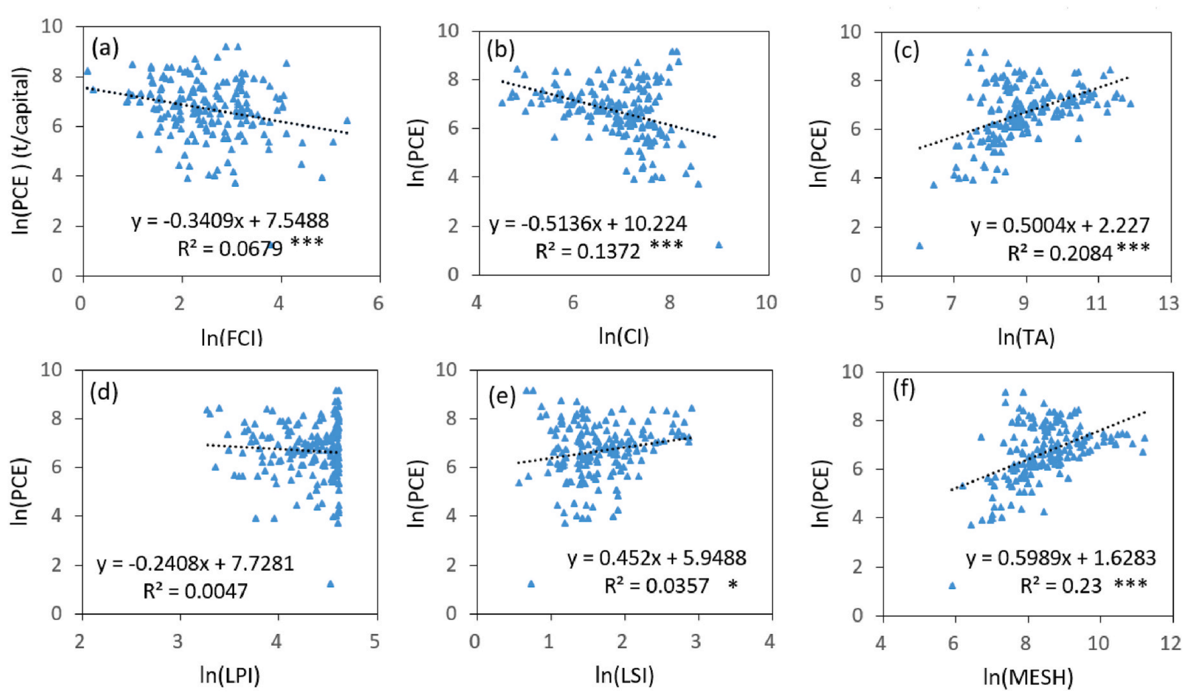

Fig. 6. Relationship between urban form metrics and the intensity of urban CO_2 emissions. Note: * (***) indicates that the results are significant at the 0.05 (0.001) level.

the poorly fitting form indicators, TCE has six indicators in five categories, and PCE has five indicators in four categories. Table 2 compares the results obtained by the GWR and OLS models. For all GWR models, the AICc values are smaller than for the OLS models, with the difference between them amounting to over three, and the GWR model has larger values of R^2. Moran's I shows that the residuals of all models are randomly distributed in space, which means that the GWR model fits well.

Relationship between TCE and urban form. For urban compactness, FCI and CI reduceTCE in all cities, which is consistent with the results on the national level. The effect of FCI on TCE tends to be high in the middle and gradually decreases toward the south and north. For every 1% increase in FCI in the middle region, TCE decreases by 1.70%–2.21%. The impact is least near the Beijing-Tianjin-Hebei urban agglomeration, where TCE decrease by only 0.42%–0.68% for every 1% increase in FCI [Fig. 7(a)]. The effect of the CI on TCE is greater in the middle and gradually decreases to the south, north, east; and in the middle region: each 1% increase in the CI reduces TCE by 1.88%–2.04% [Fig. 7(b)].

The effect of TA on TCE also tends to be greater in the middle region and decreases to the south, north, and east; and in the middle region: each 1% increase in TA increases TCE by 1.40%–1.55% [Fig. 7(c)]. The LSI positively affects TCE in all cities, with a relatively larger effect in the southern cities [Fig. 7(e)]. In addition, MESH strongly (weakly) affects TCE in the south (north) [Fig. 7(f)].

Table 2
Performance of Models based on OLS and GWR.

Dependent variable	Independent variable	OLS		GWR	
		R^2	AICc	R^2	AICc
ln (CO_2)	ln (FCI)	0.21	630.08	0.52	585.22
	ln (CI)	0.54	533.01	0.72	483.85
	ln (TA)	0.64	490.16	0.76	449.53
	ln (LPI)	0.06	659.77	0.28	635.95
	ln (LSI)	0.25	619.34	0.48	584.06
	ln (MESH)	0.59	511.09	0.70	494.83
ln (PCE)	ln (FCI)	0.07	555.76	0.44	503.10
	ln (CI)	0.14	542.01	0.49	487.53
	ln (TA)	0.21	526.67	0.52	475.77
	ln (LSI)	0.04	561.81	0.41	511.58
	ln (MESH)	0.59	511.09	0.50	479.97

Relationship between PCE and urban form. Compactness, extension, irregularity, and concentration all produce bio-directional impacts on PCE. FCI and CI correlate negatively with the PCE of most cities, with the largest impact being in the middle region and then decreasing to the south and north. In the middle region, every 1% increase in the FCI reduces PCE by 0.72%–1.02%, and every 1% increase in the CI decreases PCE by 0.91%–1.24% [Fig. 7(g) and (h)]. TA correlates positively with PCE in most cities, with the largest correlation being in the middle region, where a 1% increase in TA increases PCE by 0.74%–0.98% [Fig. 7 (i)]. The LSI produces the most obvious two-way correlation with PCE, with a positive (negative) correlation with most southern (northern) cities [Fig. 7(j)]. MESH correlates positively with PCE in most cities: every 1% increase in MESH in the middle region (where the correlation is largest) increases PCE by 0.76%–0.98% [Fig. 7(k)].

4.5. Relationship between urban form and CO_2 emissions for different industrial structures

The main source of CO_2 emission is the consumption of energy, and industry is the main consumer of energy. The 178 sample cities are divided into four categories based on their 2019 share of secondary industry in the regional GDP, as determined by the natural breaks (Jenks) method. The first type of city has the lowest share of secondary industry, ranging from 0 to 30.94, and includes 27 cities. We define these as "low industrial cities." The share of secondary industry in category-two cities ranges from 30.95 to 40.90 and includes 52 cities defined as medium industrial cities. The share of secondary industry in category-three cities ranges from 40.91 to 48.90 and includes 62 cities defined as high industrial cities. Finally, the share of secondary industry in category-four cities is the highest, ranging from 48.91 to 59.11 and including 37 cities defined as extra-high industrial cities. These form indicators of different categories serve to explore the relationship between urban forms with different industrial structures and TCE and PCE.

In terms of urban compactness, both FCI and CI exhibit a significant

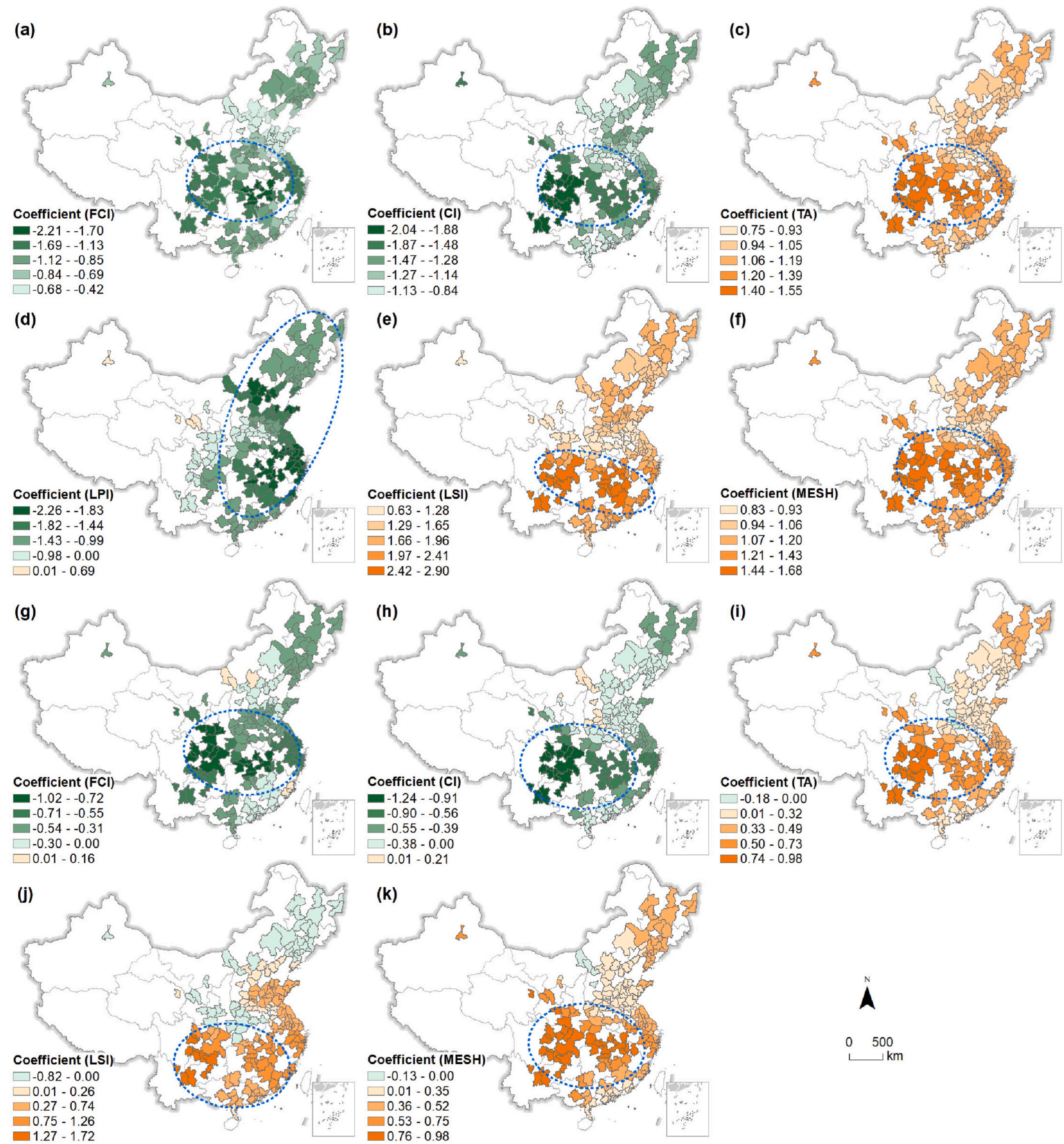

Fig. 7. Spatial distribution of coefficients. (a)–(f) Coefficients of urban form with TCE. (g)–(k) Coefficients of urban form with PCE. The blue ellipses enclose regions with strong influence. (For interpretation of the references to colour in this figure legend, the reader is referred to the Web version of this article.)

negative correlation with TCE under different secondary industry share scenarios, and clear spatial differences appear in model fit as well as in the degree of effects, with the CI having a greater overall effect on TCE than the FCI. Specifically, the FCI exhibits a stronger correlation with TCE in cities with a lower share of secondary industries, where a 1% increase in the FCI reduces TCE by 1.05% in low-industrial cities. The CI exhibits a strong negative correlation with TCE in extra-high industry cities, where a 1% increase in the CI reduces TCE by 1.58%.

Urban extension exhibits a significant positive correlation with TCE in all four categories of cities. Urban expansion has the greatest impact on extra-high industrial cities, where TCE increases by 1.38% for every 1% increase in TA. Urban fragmentation correlates negatively with all types of cities but is not statistically significant for low and medium industrial cities; it explains only 12% of the TCE in high and extra-high industrial cities. Urban irregularity exhibits a significant positive correlation with TCE in all four types of cities and is most strongly correlated with extra-high industrial cities, where a 1% increase in the LSI increases TCE by 1.79%. Urban concentration exhibits a significant positive correlation with TCE for all types of cities and is most strongly correlated with extra-high industrial cities, where a 1% increase in MESH increases TCE by 1.60% [Fig. 8(a)].

The fit between urban form and PCE in cities with different industrial structures is worse than that between urban form and TCE. In the compactness category, the FCI exhibits a significant negative correlation with PCE in medium and extra-high industrial cities, where each 1% increase in the FCI decreases PCE by 0.33% and 0.48%, respectively. The CI exhibits a significant negative correlation with high and extra-high industrial cities, where each 1% increase in the CI decreases PCE cities by 0.46% and 1.16%, respectively. Urban extension exhibits a significant positive correlation with PCE in medium, high, and extra-high industrial cities. Urban irregularity only exhibits a significant positive correlation with PCE in extra-high industrial cities. Urban concentration exhibits a significant positive correlation with PCE in all types of cities, and the greater the share of secondary industry, the greater the correlation with MESH [Fig. 8(b)].

4.6. *Effects of urban form on CO_2 emissions as a function of topographic environment and spatial structure*

In the GWR model, spatial heterogeneity appears in the correlation between urban form and TCE and PCE. Therefore, we further explore how urban form affects TCE and PCE as a function of topographic environment and spatial structure as represented by the degree of relief of land surface and polycentricity, respectively. The degree of relief of land surface refers to the difference in elevation between the highest point and the lowest point in the surface unit. In this paper, we use ASTER GDEM V3 to calculate the degree of relief of the land surface of cities and classify them into three categories by using the natural breaks (Jenks) model. The relief of category A cities (mainly plain cities) is 0–14.12 m. The relief of category B cities (mainly hilly cities) is 14.13–28.52 m. The relief of category C cities (mainly mountain cities) is 28.53–76.63 m. The urban spatial structure contains both morphological and functional categories. In this study, the morphological category is used to differentiate cities into single-center cities (S) and multi-center cities (M).

Except for the LPI, all form indicators produce an increase in TCE with increasing degree of relief of land surface; that is, the change in urban form reduces more TCE in cities with a high degree of relief of land surface. Specifically, each 1% increase in the FCI reduces TCE by 0.95%, 1.10%, and 1.30% for cities of categories A, B, and C, respectively. Each 1% increase in the CI reduces TCE by 1.26%, 1.41%, and 1.89% for cities of categories A, B, and C, respectively. Every 1% increase in the LPI reduces TCE by 1.38%, 1.30%, and 10.8% in cities of categories A, B, and C, respectively. TA and MESH produce similar effects on TCE. The LSI has the greatest impact on TCE. For every 1% increase in LSI, TCE in cities A, B, and C will increase by 1.60%, 2.03%, and 2.37%, respectively.

All form indicators produce a slightly greater impact on multi-center cities than on single-center cities; that is, adjusting the urban form is more conducive to reducing carbon emissions in multi-center cities than in single-center cities. For every 1% increase in the FCI, TCE in S and M cities decrease by 0.98% and 1.09%, respectively. For every 1% increase in the CI, TCE in S and M cities decrease by 1.31% and 1.41%, respectively. Each 1% increase in TA increases TCE by 1.11% and 1.19% in S and M cities, respectively. For each 1% increase in the LPI, TCE of S and M cities decrease by 1.27% and 1.44%, respectively. For each 1% increase in the LSI, TCE of S and M cities increases by 1.68% and 1.97%, respectively. Finally, for each 1% increase in MESH, TCE in S and M cities increases by 1.18% and 1.28%, respectively (Fig. 9).

The impact of urban form on PCE is slightly smaller than that of urban form on TCE. FCI, CI, TA, LSI and MESH produce an increase in PCE with increasing degree of relief of land surface. For every 1% increase in the FCI, PCE in cities A, B, C decreases by 0.40%, 0.44% and 0.72%, respectively. For every 1% increase in the CI, PCE in cities A, B, C decreases by 0.32%, 0.53% and 0.99%, respectively. For every 1% increase in the TA, PCE in cities A, B, C increases by 0.31%, 0.49% and 0.85%, respectively. Each 1% increase in LSI increases PCE by 0.24%, 0.63% and 1.05% in cities A, B, C, respectively. Each 1% increase in MESH increases PCE by 0.37%, 0.55% and 0.92% in cities A, B, C, respectively.

For every 1% increase in the FCI, PCE in cities S and M decreases by 0.43%, 0.44%, respectively. For every 1% increase in the CI, PCE in cities S and M decreases by 0.39%, 0.50%, respectively. For every 1% increase in the TA, PCE in cities S and M increases by 0.36%, 0.46%, respectively. Each 1% increase in LSI increases PCE by 0.34%, 0.56% in cities S and M, respectively. Finally, each 1% increase in MESH increases PCE by 0.42%, 0.53% in cities S and M, respectively (Fig. 10).

5. Discussion

5.1. *Role of urban functional form in carbon emission reduction*

The FCI correlates negatively with TCE and PCE; that is, the more compact the urban functions, the lower the CO_2 emissions. This is because the more compact urban function means that the intensity of human activities between residential zones and the remaining zones is greater, and a shorter average distance between residential zones and other zones, and less infrastructure such as urban roads, drainage pipes,

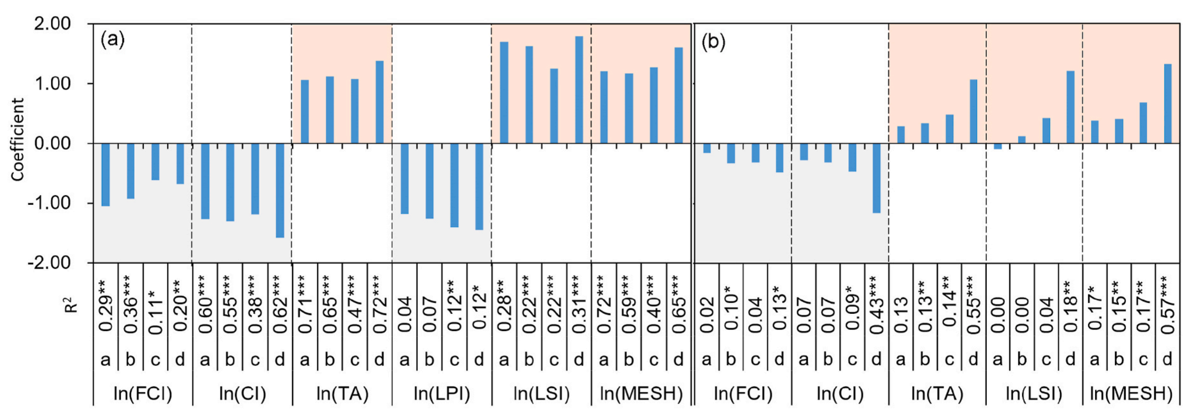

Fig. 8. Relationship between urban form and TCE and PCE in cities with different shares of secondary industry. (a) Relationship between urban form and TCE for various shares of secondary industry. (b) Relationship between urban form and PCE for various shares of secondary industry. Note: *, **, and *** indicate that the results are significant at the 0.05, 0.01, and 0.001 levels, respectively. Panels (a)–(d) are for low, medium, high, and extra-high industrial cities.

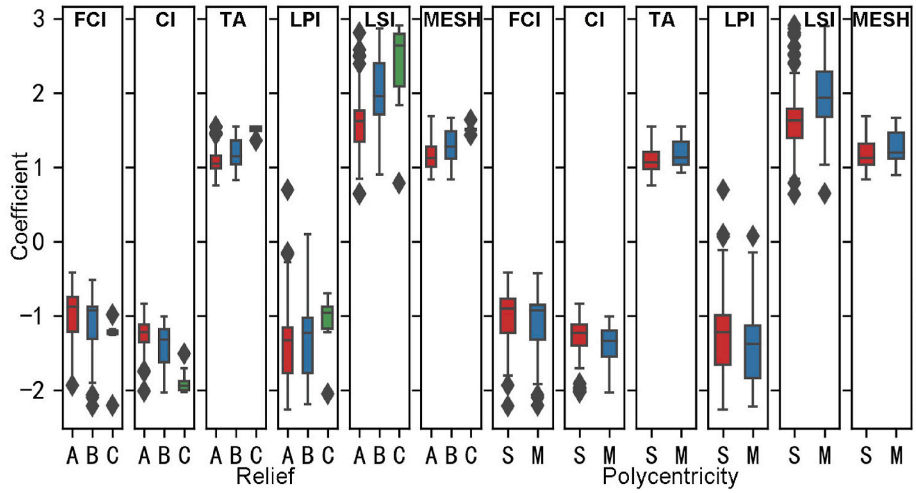

Fig. 9. Spatial heterogeneity of the influence of urban form on TCE. A indicates cities with degree of relief of land surface of 5.40–14.12 m, B indicates cities with degree of relief of land surface of 14.13–28.52 m, C indicates cities with degree of relief of land surface of 28.53–76.63 m, S indicates single-center cities, and M indicates multi-center cities.

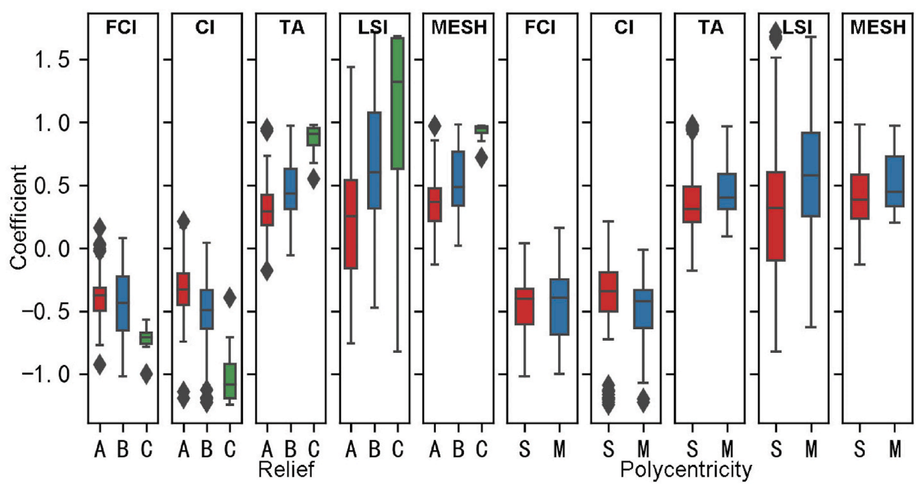

Fig. 10. Spatial heterogeneity of the influence of urban form on PCE.

water supply pipes, etc., thereby reducing CO_2 emissions from infrastructure as well as traffic, and lowing the CO_2 emissions (Schwanen, 2021; Zhu et al., 2022).

Optimizing the layout of urban functions and improving urban functional compactness have both theoretical and practical significance for reducing CO_2 emissions. In recent years, urban regeneration has been a subject of focus in the field of urban planning and construction in China. Urban regeneration has as goal to prevent urban sprawl by sustainably improving the spatial form and function within the existing urban boundaries. It is vital to optimize the urban layout within existing boundaries and improve urban functional compactness to reduce CO_2 emissions.

Table 3 lists measures, based on experience, to reduce urban carbon emissions by adjusting different form categories. Specifically, measures to reduce carbon emissions by leveraging the categories of urban extension and concentration are (i) to reduce the urban area and (ii) to reduce the fraction of the largest patch area, respectively. The measures to reduce carbon emissions by leveraging fragmentation and irregularity are (i) to reduce the fragmentation of urban form and (ii) to reduce the complexity of cities, respectively. However, within the constraint of physical terrain, it is difficult to reduce urban carbon emissions in a short period of time by reducing urban areas or simplifying complex boundaries.

From the perspective of compactness, shortening the average distance between urban plots and increasing the area of internal construction land both reduce carbon emissions by exploiting physical compactness, but blindly increasing the construction land within a city may reduce the green space within the city where residents can rest and relax, thus lowering the quality of life of residents (Vaccari et al., 2013). Thus, from the perspective of functional compactness, the measures for reducing carbon emissions include adjusting the layout of urban functional areas, shortening the average travel distance of residents, and increasing the intensity of human activities. These measures are more in line with the goal of sustainable development. Therefore, improving the compactness of urban functions to reduce carbon emissions is of vital practical significance.

5.2. Compact development is more conducive to reducing urban carbon emissions

What type of urban form is conducive to the sustainable development of cities? Through quantitative analysis we find that a compact urban form is more helpful to reduce the carbon emission of cities. The FCI and CI, which are two indicators of urban compactness, exhibit a significant

Table 3
Measures for reducing carbon emissions using different form categories.

Category	Indicator	Relationship with TCE	Relationship with PCE	Measure
Compactness	FCI	–	–	Adjusting the layout of urban functional areas; Shortening the average travel distance of residents; Increasing the intensity of human activities
	CI	–	–	Shortening the average distance between urban patches; Increasing construction land within the city
Extension	TA	+	+	Reducing urban area
Fragmentation	LPI	–		Reducing urban fragmentation
Irregularity	LSI	+	+	Reducing urban complexity
Concentration	MESH	+	+	Reducing the proportion of the largest urban patches

negative correlation with TCE on both the national and local levels and for different industrial structures; that is, the more compact the city, the lower the TCE. The FCI and CI are also negatively correlated with PCE on a national level and for different industrial structures and are negatively correlated with most cities on the local level. Urban extension, fragmentation, and irregularity correlate positively with TCE and PCE of most cities, which is consistent with the results of existing research (Ou et al., 2013; Shi et al., 2020; Vaccari et al., 2013; Wang et al., 2017). Since larger cities in China tend to be economically developed, with higher population densities, more infrastructure (e.g., roads), more cars, and more energy consumption, which inevitably increases TCE and PCE. More urban fragmentation and complexity renders it more difficult to reasonably arrange urban functional areas, so roads become more complex, which increases CO_2 emissions. The increase in urban concentration also increases CO_2 emissions, which differs from the results of existing research (Wang et al., 2018a). A possible reason is that cities with large MESH values generally have more developed economies and larger populations, so they produce more CO_2 emissions. Thus, compact development can help reduce urban CO_2 emissions.

In addition, since the physical form of a city is limited by topography and landscape, the layout of the functional areas can only be adjusted within the given physical form, which allows the physical compactness CI to have a greater impact on TCE and PCE. For example, Chongqing developed under the natural geographical pattern of "four mountains, three valleys, and two rivers." The physical space for development was very limited. Given the limitation of natural geography, the layout of urban functions is also limited, resulting in the complexity of urban transportation in Chongqing, which is one of the reasons for its high TCE.

5.3. Develop regionally differentiated carbon reduction policies

In the relationship between urban form and PCE, all categories increase PCE with increasing industrial share. Therefore, the form control of extra-high industrial cities should focus on the comprehensive adjustment of various categories, strictly control city size, and concentrate on urban regeneration within the city. Low industrial cities should focus on optimizing urban functional layout and appropriately increase city level.

Adjusting the urban form is more beneficial to reducing carbon emissions in cities with a greater degree of relief of land surface. The influence of urban form on TCE and PCE increases with increasing degree of relief of land surface. A possible reason for this is that the greater is the degree of relief of a city, the greater its physical form is constrained, and the more complex are its streets (Yang et al., 2021), resulting in greater CO_2 emissions. In this case, adjusting the urban form is more conducive to reducing carbon emissions.

In different topographic environments, the LSI has the greatest impact on TCE, but the strongest impact on PCE differs. The FCI has the greatest impact on class A cities with the lowest degree of relief, and the LSI has the greatest impact on class B and C cities. Therefore, in plain cities, more attention should focus on improving urban functional form, whereas, in hilly and mountainous cities, more attention should focus on adjusting the urban form complexity.

Adjusting the urban form is more conducive to reducing the carbon emissions of multi-center cities. The impact of urban form on TCE and PCE is slightly greater in multi-center cities than in single-center cities. Cirilli and Veneri (2013) reported that fewer urban centers correlate with less CO_2 emissions generated by commuting, and the PCE in single-center cities is lower than that in multi-center cities. With the expansion of cities, cities develop from single-center to multi-center, and CO_2 emissions increase. For multi-center cities, a reasonable urban form is conducive to carbon emission reduction. The best form of the city comes from considering the urban spatial structure and giving priority to the planning and control of the urban form in the big multi-center cities, whereas controlling the form of small and medium-sized cities is less important, provided they are still in the single-center stage.

5.4. Uncertainty and prospects

The CO_2 emissions data is the basis for the analysis in this study, and CO_2 emissions data are likely to introduce uncertainty of the results. Recently, The urban emissions in near-real-time Global Gridded Daily CO_2 emissions Dataset (GRACED) produced by Dou et al. (2022) have the merit of high-quality, fine-grained and near-real-time. Here we analyzed the relationship between CO_2 emissions of GRACED and eight form metrics revealed similar findings (Fig. 11), which further supports the conclusions of this study.

The quantitative relationship between CO_2 emissions from different sources and different categories of urban form needs to be further explored in future studies in conjunction with more finely disaggregated CO_2 emissions data to make more detailed scientific policies. In addition, the urban form indicators selected herein mainly measure the two-dimensional characteristics of urban form, which cannot reflect the three-dimensional characteristics of urban space. However, the different three-dimensional characteristics of urban form may also lead to differences in CO_2 emissions. For example, although high-rise buildings may conserve land area, they increase CO_2 emissions due to the extensive use of building equipment such as elevators, water supply pipes, and drainage pipes. The relationship between the urban form in three-dimensional space and CO_2 emissions is worth further investigation.

6. Conclusion

This work investigates the relationship between urban form and CO_2 emissions from multiple categories, especially the urban functional form. In addition, the differences in the influence of form categories are analyzed in terms of industrial structure, topographic environment, and spatial structure to comprehensively explore the association between different categories of urban form and urban carbon emissions and to provide policy suggestions for urban emission reduction.

The results indicate that compact urban form, including physical and functional, helps to reduce carbon emissions of cities. The adjustment of

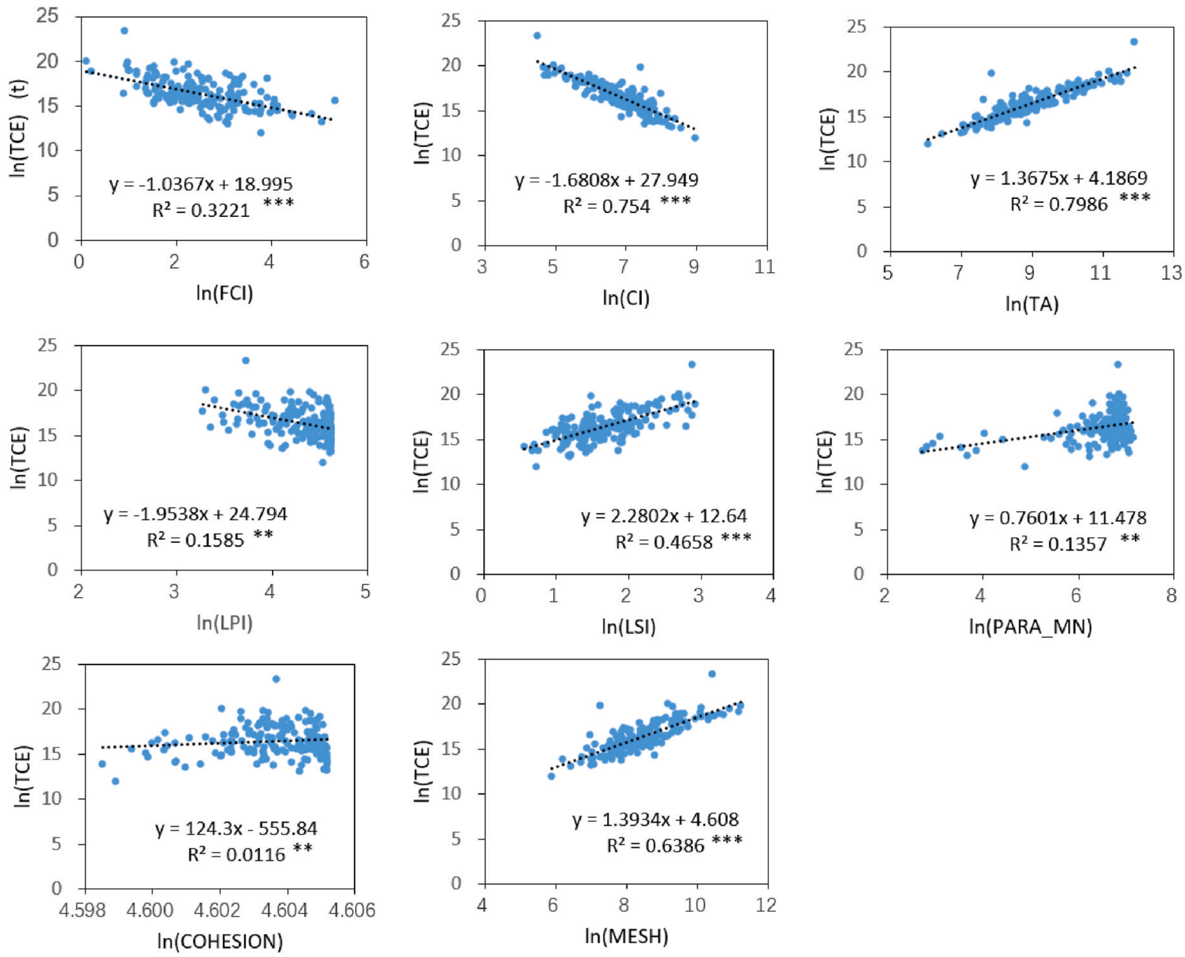

Fig. 11. Relationship between urban form indicators and TCE in GRACED. Note: ** (***) indicates that the results are significant at the 0.01 (0.001) level.

the urban functional form has important theoretical and practical significance for urban carbon reduction as it is more feasible to adjust the layout of urban functional areas within the existing urban boundaries than measures such as reducing urban area.

In addition, carbon emission reduction policies should be tailored to local conditions, consider the topographical environment, spatial structure, and industrial structure of cities, and prioritize the planning and control of urban forms in hilly and mountainous cities, large multi-center cities, and highly industrial cities. In addition to developing technology, using clean energy, and improving energy efficiency, adjusting urban functional form is an effective way to reduce urban CO_2 emissions while maintaining urban economic development.

The results of this work have important theoretical and practical significance for China to achieve the goal of carbon peaking before 2030 and carbon neutrality before 2060. The paper makes the following three main contributions: First, we empirically quantify the relationship between urban functional form and carbon emissions; second, we help to identify the important factors of CO_2 emissions in urban form; and third, we provide policy recommendations based on adjusting urban form to achieve low-carbon cities.

Credit author statement

Ting Lan: Conceptualization, Methodology, Software, Data curation, Writing – original draft, Visualization, Investigation, Validation, Writing- Reviewing and Editing. **Guofan Shao**: Supervision, Writing- Reviewing and Editing. **Zhibang Xu**: Methodology, Software, Writing- Reviewing and Editing. **Lina Tang**: Conceptualization, Methodology, Supervision, Writing- Reviewing and Editing. **Hesong Dong**: Writing- Reviewing and Editing

Declaration of competing interest

The authors declare that they have no known competing financial interests or personal relationships that could have appeared to influence the work reported in this paper.

Data availability

Data will be made available on request.

Acknowledgment

This research was funded by the National Natural Science Foundation of China (41471137), and the Strategic Priority Research Program (A) of the Chinese Academy of Sciences (XDA23030104).

References

Anderson, W.P., Kanaroglou, P.S., Miller, E.J., 1996. Urban form, energy and the environment: a review of issues, evidence and policy. Urban Stud. 33 (1), 7–35, 10.1080%2F00420989650012095.

Baur, A.H., Förster, M., Kleinschmit, B., 2015. The spatial dimension of urban greenhouse gas emissions: analyzing the influence of spatial structures and LULC patterns in European cities. Landsc. Ecol. 30 (7), 1195–1205. https://doi.org/10.1007/s10980-015-0169-5.

Bereitschaft, B., Debbage, K., 2013. Urban form, air pollution, and CO_2 emissions in large U.S. Metropolitan areas. Prof. Geogr. 65 (4), 612–635. https://doi.org/10.1080/00330124.2013.799991.

Cai, M., Shi, Y., Ren, C., Yoshida, T., Yamagata, Y., Ding, C., Zhou, N., 2021. The need for urban form data in spatial modeling of urban carbon emissions in China: a critical review. J. Clean. Prod. 319 https://doi.org/10.1016/j.jclepro.2021.128792.

Cao, F., Qiu, Y., Wang, Q., Zou, Y., 2022. Urban form and function optimization for reducing carbon emissions based on crowd-sourced spatio-temporal data. Int. J. Environ. Res. Publ. Health 19 (17). https://doi.org/10.3390/ijerph191710805.

Cirilli, A., Veneri, P., 2013. Spatial structure and carbon dioxide (CO_2) emissions due to commuting: an analysis of Italian urban areas. Reg. Stud. 48 (12), 1993–2005. https://doi.org/10.1080/00343404.2013.827333.

Clark, P.U., Shakun, J.D., Marcott, S.A., Mix, A.C., Eby, M., Kulp, S., Levermann, A., Milne, G.A., Pfister, P.L., Santer, B.D., Schrag, D.P., Solomon, S., Stocker, T.F., Strauss, B.H., Weaver, A.J., Winkelmann, R., Archer, D., Bard, E., Goldner, A., Lambeck, K., Pierrehumbert, R.T., Plattner, G.-K., 2016. Consequences of twenty-first-century policy for multi-millennial climate and sea-level change. Nat. Clim. Change 6 (4), 360–369. https://doi.org/10.1038/nclimate2923.

Dou, X., Wang, Y., Ciais, P., Chevallier, F., Davis, S.J., Crippa, M., Janssens-Maenhout, G., Guizzardi, D., Solazzo, E., Yan, F., Huo, D., Zheng, B., Zhu, B., Cui, D., Ke, P., Sun, T., Wang, H., Zhang, Q., Gentine, P., Deng, Z., Liu, Z., 2022. Near-real-time global gridded daily CO_2 emissions. Innovation 3 (1), 100182. https://doi.org/10.1016/j.xinn.2021.100182.

Elvidge, C.D., Zhizhin, M., Ghosh, T., Hsu, F.-C., Taneja, J., 2021. Annual time series of global VIIRS nighttime lights derived from monthly averages: 2012 to 2019. Remote sens 13 (5). https://doi.org/10.3390/rs13050922.

Fang, C., Wang, S., Li, G., 2015. Changing urban forms and carbon dioxide emissions in China: a case study of 30 provincial capital cities. Appl. Energy 158, 519–531. https://doi.org/10.1016/j.apenergy.2015.08.095.

Gaigne, C., Riou, S., Thisse, J.-F., Working Paper Series, G., 2010. Are compact cities environmentally friendly? SSRN Electron. J. https://doi.org/10.2139/ssrn.1553776.

GEA, 2012. Global Energy Assessment – toward a Sustainable Future. Cambridge University Press, Cambridge, UK.

Guo, R., Leng, H., Yuan, Q., Song, S., 2022. Impact of urban form on CO_2 emissions under different socioeconomic factors: evidence from 132 small and medium-sized cities in China. Land 11 (5). https://doi.org/10.3390/land11050713.

Hansen, J., Lebedeff, S., 1987. Global trends of measured surface air temperature. JGR 92 (D11). https://doi.org/10.1029/JD092iD11p13345.

IEA, 2012. World Energy Outlook 2012. International Energy Agency (IEA), Paris.

Jia, Y.Q., Tang, L.N., Xu, M., Yang, X.Y., 2019. Landscape pattern indices for evaluating urban spatial morphology – a case study of Chinese cities. Ecol. Indicat. 99, 27–37. https://doi.org/10.1016/j.ecolind.2018.12.007.

Jiao, L.M., Xu, Z.B., Xu, G., Zhao, R., Liu, J.F., Wang, W.L., 2020. Assessment of urban land use efficiency in China: a perspective of scaling law. Habitat Int. 99 https://doi.org/10.1016/j.habitatint.2020.102172.

Kennedy, C.A., Ibrahim, N., Hoornweg, D., 2014. Low-carbon infrastructure strategies for cities. Nat. Clim. Change 4 (5), 343–346. https://doi.org/10.1038/nclimate2160.

Khanna, N., Fridley, D., Hong, L., 2014. China's pilot low-carbon city initiative: a comparative assessment of national goals and local plans. Sustain. Cities Soc. 12, 110–121. https://doi.org/10.1016/j.scs.2014.03.005.

Lan, T., Shao, G., Xu, Z., Tang, L., Sun, L., 2021. Measuring urban compactness based on functional characterization and human activity intensity by integrating multiple geospatial data sources. Ecol. Indicat. 121 https://doi.org/10.1016/j.ecolind.2020.107177.

Li, Z., Wu, H., Wu, F., 2022. Impacts of urban forms and socioeconomic factors on CO_2 emissions: a spatial econometric analysis. J. Clean. Prod. 372 https://doi.org/10.1016/j.jclepro.2022.133722.

Liu, H., Huang, B., Zhan, Q., Gao, S., Li, R., Fan, Z., 2021a. The influence of urban form on surface urban heat island and its planning implications: evidence from 1288 urban clusters in China. Sustain. Cities Soc. 71 https://doi.org/10.1016/j.scs.2021.102987.

Liu, X., Ou, J., Wang, S., Li, X., Yan, Y., Jiao, L., Liu, Y., 2018. Estimating spatiotemporal variations of city-level energy-related CO2 emissions: an improved disaggregating model based on vegetation adjusted nighttime light data. J. Clean. Prod. 177, 101–114. https://doi.org/10.1016/j.jclepro.2017.12.197.

Liu, Y., Huang, L., Onstein, E., 2020. How do age structure and urban form influence household CO_2 emissions in road transport? Evidence from municipalities in Norway in 2009, 2011 and 2013. J. Clean. Prod. 265 https://doi.org/10.1016/j.jclepro.2020.121771.

Liu, Y., Song, Y., Song, X., 2014. An empirical study on the relationship between urban compactness and CO_2 efficiency in China. Habitat Int. 41, 92–98. https://doi.org/10.1016/j.habitatint.2013.07.005.

Liu, Z., Deng, Z., He, G., Wang, H., Zhang, X., Lin, J., Qi, Y., Liang, X., 2021b. Challenges and opportunities for carbon neutrality in China. Nat. Rev. Earth Environ. https://doi.org/10.1038/s43017-021-00244-x.

Makido, Y., Dhakal, S., Yamagata, Y., 2012. Relationship between urban form and CO_2 emissions: evidence from fifty Japanese cities. Urban Clim. 2, 55–67. https://doi.org/10.1016/j.uclim.2012.10.006.

Oda, T., Maksyutov, S., 2011. A very high-resolution (1 km$\times$1 km) global fossil fuel CO_2 emission inventory derived using a point source database and satellite observations of nighttime lights. Atmos. Chem. Phys. 11 (2), 543–556. https://doi.org/10.5194/acp-11-543-2011.

Oda, T., Maksyutov, S., Andres, R.J., 2018. The Open-source Data Inventory for Anthropogenic CO_2, version 2016 (ODIAC2016): a global monthly fossil fuel CO_2 gridded emissions data product for tracer transport simulations and surface flux inversions. Earth Syst. Sci. Data 10 (1), 87–107. https://doi.org/10.5194/essd-10-87-2018.

Ou, J., Liu, X., Li, X., Chen, Y., 2013. Quantifying the relationship between urban forms and carbon emissions using panel data analysis. Landsc. Ecol. 28 (10), 1889–1907. https://doi.org/10.1007/s10980-013-9943-4.

Rosenzweig, C., Solecki, W., Hammer, S.A., Mehrotra, S., 2010. Cities lead the way in climate-change action. Nature 467 (7318), 909–911. https://doi.org/10.1038/467909a.

Schwanen, T., 2021. Achieving just transitions to low-carbon urban mobility. Nat. Energy 6 (7), 685–687. https://doi.org/10.1038/s41560-021-00856-z.

Sha, W., Chen, Y., Wu, J., Wang, Z., 2020. Will polycentric cities cause more CO_2 emissions? A case study of 232 Chinese cities. J. Environ. Sci. (China) 96, 33–43. https://doi.org/10.1016/j.jes.2020.04.025.

Shi, K., Xu, T., Li, Y., Chen, Z., Gong, W., Wu, J., Yu, B., 2020. Effects of urban forms on CO_2 emissions in China from a multi-perspective analysis. J. Environ. Manag. 262, 110300 https://doi.org/10.1016/j.jenvman.2020.110300.

Smith, S.J., Edmonds, J., Hartin, C.A., Mundra, A., Calvin, K., 2015. Near-term acceleration in the rate of temperature change. Nat. Clim. Change 5 (4), 333–336. https://doi.org/10.1038/nclimate2552.

Sun, L., Tang, L., Shao, G., Qiu, Q., Lan, T., Shao, J., 2019. A machine learning-based classification system for urban built-up areas using multiple classifiers and data sources. Remote sens 12 (1). https://doi.org/10.3390/rs12010091.

Thinh, N.X., Arlt, G., Heber, B., Hennersdorf, J., Lehmann, I., 2002. Evaluation of urban land-use structures with a view to sustainable development. Environ. Impact Assess. Rev. 22 (5), 475–492. https://doi.org/10.1016/s0195-9255(02)00023-9.

Tollefson, J., 2021. IPCC climate report: Earth is warmer than it's been in 125,000 years. Nature 596 (7871), 171–172. https://doi.org/10.1038/d41586-021-02179-1.

Vaccari, F.P., Gioli, B., Toscano, P., Perrone, C., 2013. Carbon dioxide balance assessment of the city of Florence (Italy), and implications for urban planning. Landsc. Urban Plann. 120, 138–146. https://doi.org/10.1016/j.landurbplan.2013.08.004.

Wang, H., Lu, X., Deng, Y., Sun, Y., Nielsens, C.P., Li, Y., Zhu, G., Bu, M., Bi, J., McElroy, M.B., 2019a. China's CO_2 peak before 2030 implied from characteristics and growth of cities. Nat. Sustain. 2 (8), 748–754. https://doi.org/10.1038/s41893-019-0339-6.

Wang, S., Liu, X., Zhou, C., Hu, J., Ou, J., 2017. Examining the impacts of socioeconomic factors, urban form, and transportation networks on CO_2 emissions in China's megacities. Appl. Energy 185, 189–200. https://doi.org/10.1016/j.apenergy.2016.10.052.

Wang, S., Shi, C., Fang, C., Feng, K., 2019b. Examining the spatial variations of determinants of energy-related CO_2 emissions in China at the city level using Geographically Weighted Regression Model. Appl. Energy 235, 95–105. https://doi.org/10.1016/j.apenergy.2018.10.083.

Wang, S., Wang, J., Fang, C., Li, S., 2018a. Estimating the impacts of urban form on CO_2 emission efficiency in the Pearl River Delta, China. Cities 85, 117–129. https://doi.org/10.1016/j.cities.2018.08.009.

Wang, S.H., Huang, S.L., Huang, P.J., 2018b. Can spatial planning really mitigate carbon dioxide emissions in urban areas? A case study in Taipei, Taiwan. Landsc. Urban Plann. 169, 22–36. https://doi.org/10.1016/j.landurbplan.2017.08.001.

Williams, K., 2014. Urban Form and Infrastructure: a Morphological Review. Foresight, Government Office for Science, London.

Xu, Z., Jiao, L., Lan, T., Zhou, Z., Cui, H., Li, C., Xu, G., Liu, Y., 2021. Mapping hierarchical urban boundaries for global urban settlements. Int. J. Appl. Earth Obs. Geoinf. 103 https://doi.org/10.1016/j.jag.2021.102480.

Yang, N., Jiang, L., Chao, Y., Li, Y., Liu, P., 2021. Influence of relief degree of land surface on street network complexity in China. ISPRS Int. J. Geo-Inf. 10 (10) https://doi.org/10.3390/ijgi10100705.

Yao, F., Zhu, H., Wang, M., 2021. The impact of multiple dimensions of urbanization on CO_2 emissions: a spatial and threshold analysis of panel data on China's prefecture-level cities. Sustain. Cities Soc. 73 https://doi.org/10.1016/j.scs.2021.103113.

Zhang, W., Huang, B., Luo, D., 2014. Effects of land use and transportation on carbon sources and carbon sinks: a case study in Shenzhen, China. Landsc. Urban Plann. 122, 175–185. https://doi.org/10.1016/j.landurbplan.2013.09.014.

Zhu, X.H., Lu, K.F., Peng, Z.R., He, H.D., Xu, S.Q., 2022. Spatiotemporal variations of carbon dioxide (CO_2) at Urban neighborhood scale: characterization of distribution patterns and contributions of emission sources. Sustain. Cities Soc. 78 https://doi.org/10.1016/j.scs.2021.103646.

Zuo, S., Dai, S., Ju, J., Meng, F., Ren, Y., Tian, Y., Wang, K., 2022. The importance of the functional mixed entropy for the explanation of residential and transport CO_2 emissions in the urban center of China. J. Clean. Prod. 380, 134947.